Original Articles

Linkages between bacterial community and extracellular enzyme activities crossing a coastal front

Shujie Cai [a], Feipeng Wang [b], Edward A. Laws [c], Yao Liu [a], Chao Xu [a], Lingqi Ma [a], Wupeng Xiao [a,*], Bangqin Huang [a]

[a] State Key Laboratory of Marine Environmental Science, Fujian Provincial Key Laboratory for Coastal Ecology and Environmental Studies, College of the Environment and Ecology, Xiamen University, Xiamen 361102, China
[b] Fujian Key Laboratory on Conservation and Sustainable Utilization of Marine Biodiversity, Fuzhou Institute of Oceanography, Minjiang University, Fuzhou 350108, China
[c] Department of Environmental Sciences, College of the Coast & Environment, Louisiana State University, Baton Rouge, LA 70803, USA

ABSTRACT

Exploring the responses of microbial communities and their functions to marine frontal systems are the foci of marine ecologists. However, most of the existing studies have focused on only microbial communities or their functions. The relationships between microbial communities and their functions across coastal fronts therefore remain unclear. Here we studied a coastal front in the Taiwan Strait during late spring and examined the bacterial community structure, extracellular enzymatic activity (EEA), and their linkages. The results showed that the coastal front strongly delineated zones of bacterial community composition and diversity and functioned as a transitional zone rather than a hotspot between the coastal water and offshore water. Co-occurrence network analysis indicated that the interaction of bacterial communities was much weaker in the frontal zone than in the water masses on both sides. The suggestion was that the highly fluctuating environment in the frontal zone reduced the complexity and stability of the bacterial co-occurrence network. The activities of β-glucosidase (BGA) and leucine aminopeptidase (LAPA) were as high in the frontal zone as in the coastal water and much higher than those in offshore waters. We therefore suggest that, despite obvious shifts in the bacterial community structure in the frontal zone, the bacterial community was able to maintain its ability to hydrolyze organic substrates via functional redundancy. The composition of key microbial assemblies differed among the three water masses, and the relative abundance of module 2 in the frontal zone was positively correlated with BGA and LAPA. The indication was that changing the bacterial assemblage was the mechanism that made it possible for the bacterial community to maintain EEA in the frontal zone. Our results help to improve understanding on how bacterial community-function linkages vary in marine frontal systems.

1. Introduction

The coastal ocean is a vital interface between terrestrial and marine ecosystems and is intensely influenced by human activities (Barbier et al., 2011; Lefcheck et al., 2018). Fluvial discharges and coastal currents create natural heterogeneity and the close coexistence of coastal-eutrophic and open-oligotrophic features in coastal regions (Monticelli et al., 2014; Terhaar et al., 2021). When water masses with distinctly different environmental properties (e.g. temperature, salinity, nutrients, light) meet, strong physical and chemical gradients form on scales ranging from coastal fronts to fine spatial scales (Belkin et al., 2009; Li

et al., 2021; Monticelli et al., 2014). The abrupt variations of environmental conditions across fronts may have dramatic impacts on biological processes. For example, fronts may act as soft barriers that divide species habitats or enhance phytoplankton diversity and productivity (Gildor et al., 2009; McGillicuddy, 2016; Ribalet et al., 2010). However, because of the highly dynamic nature of coastal fronts, our understanding of their biological effects is still very poor. That poor understanding has hindered our systematical understanding of biogeochemical processes in coastal ecosystems.

Bacterioplankton play a critical role in the marine carbon cycle through remineralization and transformation of large amounts of

---

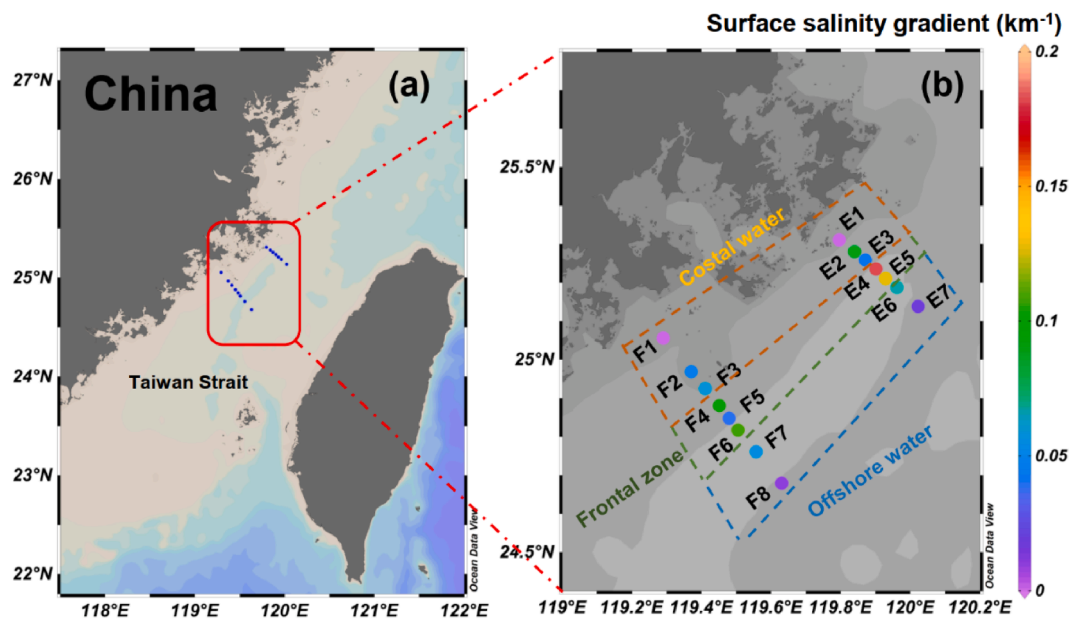**Fig. 1.** The area shown in the red box in panel (a) is the location of the study area in the Taiwan Strait. Panel (b) shows the sampling stations and the change of the salinity gradient (the ratio of the difference between the salinity of water samples to the sampling distance, km^{-1}). According to the project funding scheme supporting this study, the two transects were named E and F, respectively. (For interpretation of the references to colour in this figure legend, the reader is referred to the web version of this article.)

organic matter (Azam and Malfatti, 2007; Buchan et al., 2014). The bacterial communities first produce extracellular enzymes to hydrolyze high-molecular-weight dissolved organic matter (DOM) to smaller molecules and then transport the small hydrolysates across their cell membranes (Arnosti, 2011). Understanding the linkage between bacterial communities and extracellular enzyme activities (EEA) is needed to identify the factors that potentially regulate the fate of semi-labile DOM. However, bacterioplankton exhibit enormous genetic diversity (Azam and Malfatti, 2007), and many taxonomically distinct microbes can encode the same metabolic functions (Louca et al., 2018). This diverse functional redundancy makes the relationship between bacterial communities and enzymatic functions highly complicated. The enzymatic capacity and community composition of bacteria also affect each other, because the mineralization ability of each bacterial group is distinct, and variations of enzyme activity caused by the external environment can also alter the community composition (Kellogg and Deming, 2014; Shi et al., 2019). It is worth noting that in coastal regions, especially in frontal areas, the diversity, composition, and EEA of the bacterial community are all affected by the drastically changing environment (Allen et al., 2020; Baltar et al., 2016). For instance, clear modifications of dominant bacterial taxa and transitional variations of diversity have been confirmed in the frontal region formed by the encounter of cold, nutrient-rich sub-Antarctic waters and nutrient-poor, saline, subtropical waters along the southeast coast of New Zealand (Baltar et al., 2016; Morales et al., 2018). Also, an investigation in the Gulf of Manfredonia has revealed that the waters of the coastal thermohaline front that appears between warm, less saline coastal waters and cold, more saline offshore waters of the Adriatic Sea are characterized by distinctly different environmental conditions, and the activities of multiple extracellular enzymes such as α-glucosidase (AG), β-glucosidase (BG), and leucine aminopeptidase (LAP) differ from the corresponding activities in coastal and offshore waters (Monticelli et al., 2014). Nevertheless, despite the recognized impacts of coastal fronts on bacterial communities and EEA, these studies have usually not considered the interactions between the physics and biology. It remains unclear how the links between bacterial communities and EEA change across a coastal front.

Microorganisms form complex interactions and gather into

ecological modules or clusters according to different phylogenetic relationships and environmental preferences (Faust and Raes, 2012; Lurgi et al., 2019). Microbial communities depend on complex interactions among internal members to maintain stability and resilience to environmental disturbances (Steele et al., 2011; Wu et al., 2021). Increasing research based on network approaches has revealed the significant impact of environmental disturbances on the patterns of microbial co-occurrence (complexity, modularity, keystone taxa, and robustness) (Wu et al., 2021; Zhang et al., 2021). These network analyses have helped to not only elucidate why some microbes occur together and how the complexity and stability of microbial communities respond to changes in environmental factors but also reveal how connections between microbes affect ecosystem functioning (Fan et al., 2019; Feng et al., 2021; Qiu et al., 2021). However, it is still unclear how a coastal front impacts the complexity and stability of bacterial interactions and how the interactions among different microbial groups in the network influence key ecosystem services, such as the production of EEA.

To address this uncertainty, we performed a high-spatial-resolution study in the western coastal zone of the Taiwan Strait (TS) in the late spring of 2020 (April 30 to May 3). During that time of year, the region is known to be characterized by a coastal front formed by the interaction of the Zhe-Min Coastal Current and the Taiwan Warm Current (Li et al., 2006; Liao et al., 2018). The Zhe-Min Coastal Current is an important part of the complex current system in the coastal area of China. It originates from the Yangtze River and Hangzhou Bay. Driven by the northeast monsoon, it flows southward along the coast in winter and spring and transports nutrient-rich, continental freshwater to the south (Hong et al., 2011; Xu et al., 2020). The warm, high-salinity, oligotrophic Taiwan Warm Current flows northward. These two currents form a front when they meet in the middle of the TS (Li et al., 2006). In this study, we characterized seawater as coastal water, frontal zone water, or offshore water based on its salinity. We examined the diversity, composition, and co-occurrence patterns of the bacterial communities within these three types of seawater. We also determined the activities of two typical bacterial extracellular enzymes, BG and LAP, which are involved in carbon cycling because they catalyze the decomposition of polysaccharides and protein-derived polymers, respectively (Caruso, 2010; Shi et al., 2019). Finally, we explored the relationship between the
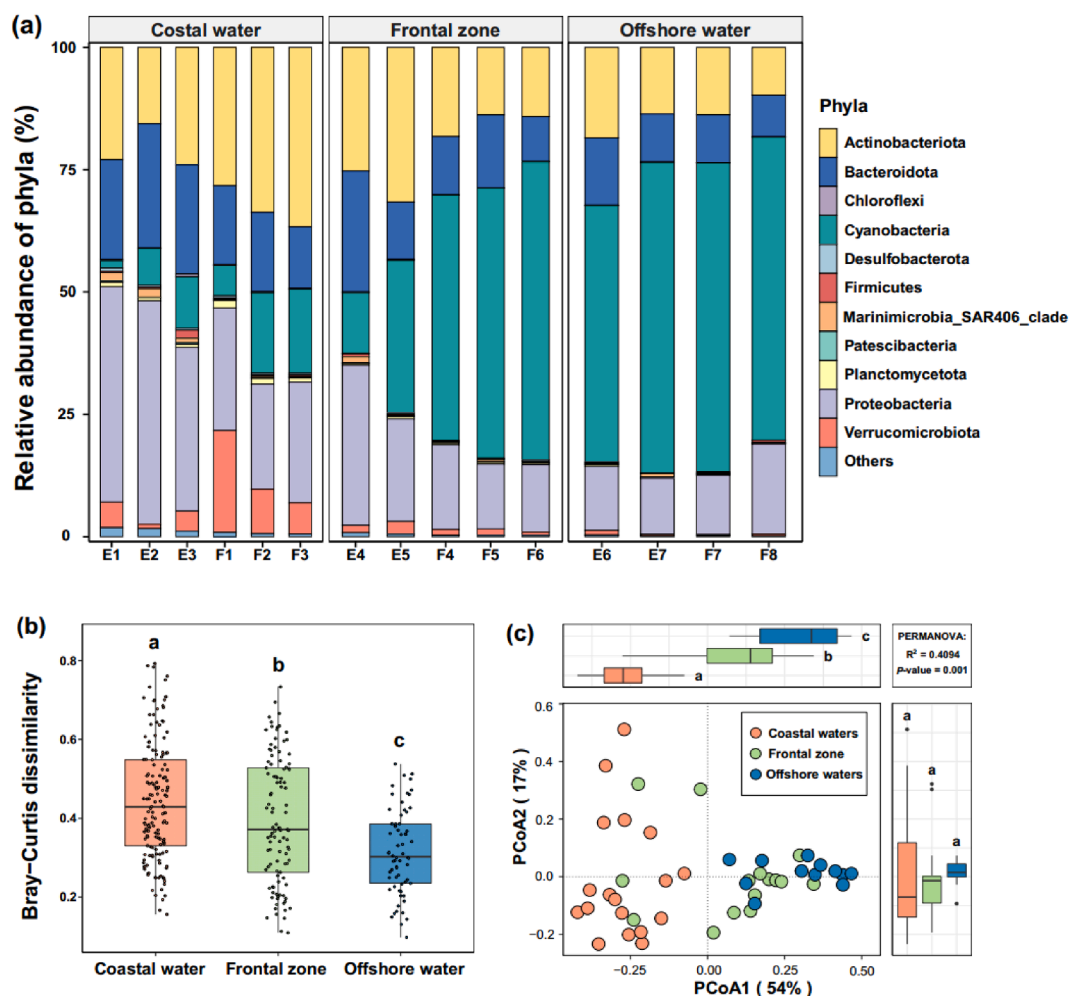
Fig. 2. Bacterial community in the coastal water, frontal zone, and offshore water. (a) The relative abundance (%) of the dominant bacterial phyla at 15 stations in May 2020. (b) Bray-Curtis dissimilarity of each water mass shows that the beta-diversity of bacterial communities was gradually lower from coastal water to offshore water. (c) Unconstrained principal coordinates analysis (PCoA) shows that the bacterial communities of each water mass have significantly distinct microbiota as detected by permutational multivariate analysis of variance (PERMANOVA).

bacterial communities and EEA. Specific goals of this project were to: i) investigate the shift across the coastal front of the diversity, composition, co-occurrence networks, and EEA of the bacterial community, and ii) explore the likely impact of the bacterial community on EEA in the frontal zone.

2. Materials and methods

2.1. Study area, sampling, and environmental parameters

To study the coastal front, we collected samples and made observations at 15 stations on two high-spatial-resolution transects (Transects E and F) in the TS during a cruise of the RV Yanping 2 from 30 April to 3 May 2020 (Fig. 1). Previous studies (Li et al., 2006; Liao et al., 2018) had indicated that during this period, these two transects would be expected to cross a coastal front generated by the intersection of the Zhe-Min Coastal Current and the Taiwan Warm Current. Niskin bottles attached to a conductivity-temperature-depth (CTD) rosette system were used to collect seawater samples. Seawater salinity and temperature were recorded during each cast with a SeaBird model SBE9/11 CTD recorder. The sea surface salinity and temperature of transects E and F ranged from 31.2−34.4 and 19.2−25.1℃, respectively, and gradients of increasing salinity and temperature from nearshore to offshore stations were apparent (Fig. S1). Following the study of Li et al. (2021), we

defined the area with a sea surface salinity gradient > 0.1 km^{-1} as the frontal zone. The water masses on the nearshore and offshore sides of the front were considered to be coastal water and offshore water, respectively (Fig. 1b). We therefore could identify three sub-areas: (1) coastal water (including stations E1, E2, E3, F1, F2, and F3) characterized by low salinity (32.1 $\pm$ 0.6) and low temperature (19.7 $\pm$ 0.4 °C); (2) offshore water (including stations E6, E7, F7, and F8) characterized by high salinity (33.4 $\pm$ 0.5) and high temperature (22.6 $\pm$ 1.8 °C); and (3) frontal zone water (including stations E4, E5, F4, F5, and F6) characterized by intermediate salinity (33.0 $\pm$ 0.3) and intermediate temperature (20.1 $\pm$ 0.5 °C) (Fig. S2a, Fig. S2b, and Fig. 1b).

A QUAATRO nutrient analyzer was used to measure inorganic nutrient concentrations, including dissolved nitrate + nitrite (NO$_x$, μmol/L), dissolved inorganic phosphorous (DIP, μmol/L), and dissolved silicon (DSi, μmol/L). The detection limits were 0.03 μmol/L, 0.02 μmol/L, and 0.05 μmol/L, respectively. Samples for the measurement of chlorophyll *a* (Chl *a*) concentrations were collected by filtering 200–500 ml of seawater through 25-mm GF/F filters (Whatman), which were then stored in liquid nitrogen. In the laboratory, the samples were submerged in 90% acetone in a dark environment at −20℃ for 16–24 h until analysis with a Trilogy fluorometer (Turner Designs, USA) (Welschmeyer, 1994).

2.2. Bacterial community

To determine bacterial diversity and community composition, triplicate seawater samples (0.5–1 L) from a depth of 3 m were collected at each sampling station. The seawater was first filtered through a 200-μm bolting cloth to remove non-target organisms. The pre-filtered seawater was then filtered through 0.22-μm pore size polycarbonate membranes. The filters were transferred to a freezer at −80 °C until analysis. The total bacterial DNA was extracted from the filters using a MOBIO Dneasy PowerSoil Kit (Qiagen, Germany). The V3–V4 region of the bacterial 16S rRNA gene was amplified using primers 338F (5′-ACTCCTACGG-GAGGCAGCAG-3′) and 806R (5′-GGACTACHVGGGTWTCTAAT-3′) with a thermocycler PCR system (GeneAmp 9700, ABI, USA) (Li et al., 2018; Liu et al., 2018). The PCR program was conducted with the following temperature cycle: denaturation at 95 °C (3 min), 27 cycles at 95 °C (30 s), annealing at 55 °C (30 s), elongation at 72 °C (45 s), and a final extension at 72 °C (10 min). PCR amplicons were extracted from 2% agarose gel and further purified with an AxyPrep DNA gel extraction kit (Axygen Biosciences, Union City, CA, USA). The purified amplicons were then placed in equimolar amounts and paired-end sequenced (2 × 300) on an Illumina MiSeq platform (Majorbio Company in Shanghai, China). All sequencing data obtained in this study have been submitted to the National Center for Biotechnology Information (NCBI) Sequence Read Archive (SRA) database under the accession number PRJNA856774.

After sequencing, the 16S rRNA gene amplicon sequences were processed with QIIME v1.9.0 (Caporaso et al., 2010) based on the following criteria: (1) over a 50-bp sliding window, 300-bp reads were truncated for any site with an average quality score below 20, and truncation reads shorter than 50-bp were abandoned; (2) two nucleotide mismatches in primer matching and reads, including ambiguous characters, were removed, and (3) sequences that overlapped by>10-bp were merged into a single sequence. Operational taxonomic units (OTUs) were clustered with a 97% similarity cutoff using UPARSE (version 7.1, https://drive5.com/uparse/) (Edgar, 2013). The Silva (SSU123) 16S rRNA database was classified using the RDP classifier algorithm (https://rdp.cme.msu.edu/) with a confidence threshold of 70%. For further analysis, OTUs assigned to chloroplasts and mitochondria were removed. To normalize the sampling effort, the OTU table in our study was rarefied to 24,965 based on the values of the minimum sequence numbers.

2.3. Co-occurrence network construction

The co-occurrence patterns of bacterial communities in the coastal water, frontal zone, and offshore water were constructed with the SparCC method (Friedman and Alm, 2012), which was implemented in the "SpiecEasi" package in R software (version 4.0.5). To select strong interactions between bacterial communities, the SparCC results were filtered on the basis of strong ($R > 0.75$) and significant ($P < 0.01$) coefficients. One thousand equal Erdős-Réyni random networks were constructed as the real networks of the three water masses (Erdős, 1960). The network topological parameters (including modularity, average clustering coefficient, average path length, and degree), node-level degree, and centrality (including closeness and eigenvector centrality) were extracted by using the "igraph" R package. The software Gephi (https://gephi.org/) was performed to visualize the final co-occurrence networks. The relative abundance of each module in all networks was calculated from the average standardized relative abundance of the species (z-score). Highly connected keystone taxa are the strong foundation of the structure of a microbial network (Banerjee et al., 2018). The role of nodes in the network was determined by the within-module connectivity Zi and the among-module connectivity Pi, which quantify the degree of connection between a node and other nodes in its module and the degree of connection between the node and different modules, respectively (Olesen et al., 2007). Specifically, nodes

were defined as peripherals (Zi < 2.5; Pi < 0.6), connectors (Zi < 2.5; Pi > 0.6), module hubs (Zi > 2.5; Pi < 0.6), and network hubs (Zi > 2.5; Pi > 0.6) (Olesen et al., 2007). The connectors, module hubs, and network hubs were considered potential keystone taxa because of their important roles in network topology (Banerjee et al., 2016). The stability of the static network was evaluated by natural connectivity, that is, the speed of robustness reduction was estimated by removing nodes of the network (Peng and Wu, 2016).

2.4. Extracellular enzyme activity

The EEA was determined using fluorescently tagged substrate analogs according to the description of Hoppe (1983). Activities of two key bacterial extracellular enzymes, BG and LAP, were estimated using 4-methylumbelliferyl-β-D-glucoside (MUF-β-D-glucoside, Sigma) and L-Leucine-7-amido-4-methylcoumarin hydrochloride (Leu-MCA, Sigma), respectively, as fluorogenic substrates (Hoppe, 1983). The MUF-β-D-glucoside and Leu-MCA were added to 3-mL seawater samples at final concentrations of 250 and 100 μmol/L, respectively. The samples were then incubated in the dark for 10 h at the in-situ temperature before the addition of 10 μL of 16-mM mercuric chloride ($HgCl_2$) to terminate the hydrolysis. The fluorescence value was measured with a fluorescence spectrophotometer (Varian, Cary Eclipse) at excitation/emission wavelengths of 365/445 nm for the activity of BG (BGA) and 380/440 nm for the activity of LAP (LAPA). Known concentrations of MUF and MCA standards were used to calibrate the velocity of substrate hydrolysis. Blank treatments (addition of the same $HgCl_2$ solution before addition of the substrate) were used to correct the value of the sample fluorescence. The net fluorescence value was used to calculate the EEA in different samples.

2.5. Statistical analyses

For each sample, bacterial alpha diversity indices, including the Shannon, Chao 1, and Pielou indices, were calculated in the R package "vegan", and the microbial beta diversities were compared based on the Bray-Curtis dissimilarity matrixes between samples. The nonparametric Wilcoxon test was performed to evaluate the differences in bacterial alpha diversity indices (Shannon, Chao 1, and Pielou), beta diversity, node-level topological properties (degree, closeness centrality, and eigenvector centrality), and EEA (BGA and LAPA) among different water masses, and the differences with $P < 0.05$ were considered to be significant. An unconstrained principal coordinate analysis (PCoA) was used to reveal the differences in bacterial community composition among water masses, and the permutation multivariate analysis of variance (PERMANOVA) test was carried out to explain the statistical significance of the differences. We then performed principal component analysis (PCA) using the "vegan" package in R to visualize the distribution pattern of the shifts in EEA and the properties of the bacterial communities. We also conducted a linear regression analysis to evaluate the relationships between the EEA and the relative abundance of the main modules in the networks.

3. Results

3.1. Environmental settings

The frontal zone, within which there were large changes of salinity, was captured by our sampling in the north-central surface waters of the TS (Fig. 1). The nutrient concentrations were high (NO_x: 3.52 ± 1.68 μmol/L, DIP: 0.08 ± 0.03 μmol/L, and DSi: 6.70 ± 2.31 μmol/L) in the coastal water and low in both the frontal zone (NO_x: 0.88 ± 0.60 μmol/L, DIP: 0.02 ± 0.60 μmol/L, and DSi: 3.71 ± 1.94 μmol/L) and offshore water (NO_x: 1.66 ± 2.60 μmol/L, DIP: 0.02 ± 0.01 μmol/L, and DSi: 2.09 ± 0.53 μmol/L) (Fig. S2c, 2d and 2e). The distribution pattern of Chl *a* differed from the physical and chemical parameters; the highest
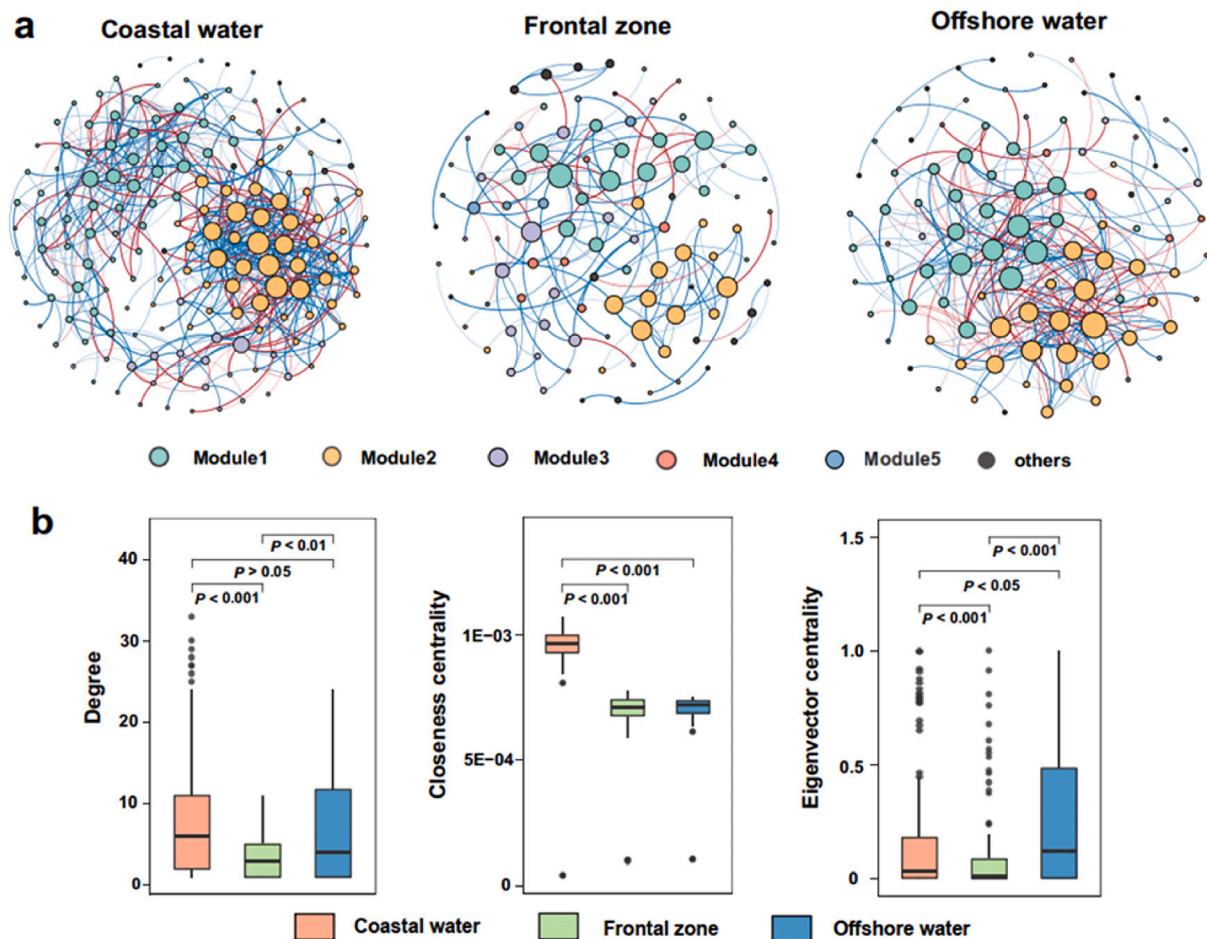
Fig. 3. Co-occurrence networks and topological properties of bacterial communities in coastal water, frontal zone, and offshore water. (a) The co-occurrence networks of the bacterial communities in coastal water, frontal zone, and offshore water. A connection represents a strong (Spearman correlation threshold $R > |0.75|$) and significant ($P < 0.01$) correlation. These three networks are colored by modular class. The red edges show negative interactions between two bacterial nodes, while the blue edges show positive interactions between two nodes. For each panel, the size of each node is proportional to the quantity of connections (degree), and the thickness of each connection between two nodes (edge) is proportional to the value of Spearman's correlation coefficients. We colored nodes that are 5% larger than the sum of nodes. (b) Comparison of node-level topological properties (degree, closeness centrality, and eigenvector centrality) in coastal water, frontal zone, and offshore water. (For interpretation of the references to colour in this figure legend, the reader is referred to the web version of this article.)

values (0.77 ± 0.34 µg L^{-1}) were found in the frontal zone (Fig. S2f).

3.2. Bacterial community composition and diversity

Obvious differences in the bacterial community composition were apparent among the three water masses (Fig. 2a). The dominant phyla in the coastal water were Proteobacteria, Actinobacteriota, and Bacteroidota. They accounted for 21.5–45.6%, 15.6–36.6%, and 12.6–25.4%, respectively, of all bacteria (Fig. 2a). The dominant phyla in the offshore water were Cyanobacteria, which accounted for 52.4–63.5% of all bacteria (Fig. 2a). The composition of the bacterial community in the

frontal zone was intermediate between the compositions of the coastal water and offshore water. The relative abundances of the dominant phyla were Cyanobacteria, Proteobacteria, Actinobacteriota, and Bacteroidota, which accounted for 12.4–60.9%, 13.3–32.8%, 13.8–31.6%, and 9.14–24.7%, respectively, of all bacteria (Fig. 2a). Results based on the Bray-Curtis dissimilarity index revealed that the beta-diversity of the bacterial community decreased significantly from the coastal water to the frontal zone (Wilcoxon test, $P < 0.05$) to the offshore water (Wilcoxon test, $P < 0.001$) (Fig. 2b). The PCoA results showed that the bacterial community compositions of the three water masses were significantly distinct in the first dimension, and the PERMANOVA

Table 1
Major topological properties of the empirical and random co-exist networks of bacterial communities in coastal water, frontal zone, and offshore water.

	Empirical networks							Random networks		
	Nodes	Edges	Modularity	Average clustering coefficient	Average Path length	Average degree	Power-law model	Modularity (SD)	Average clustering coefficient (SD)	Average path length (SD)
Coastal water	161	664	0.469	0.408	3.258	8.248	0.892	0.300 (0.008)	0.051 (0.005)	2.628 (0.007)
Frontal zone	102	175	0.694	0.368	5.366	3.431	0.919	0.506 (0.016)	0.033 (0.013)	3.759 (0.093)
Offshore water	98	333	0.399	0.388	3.282	6.796	0.869	0.323 (0.011)	0.069 (0.009)	2.581 (0.015)

A random network was generated by reconnecting all links with the same number of nodes and edges to the empirical network. The numbers in brackets represent the standard deviation (SD) of 1000 Erdös-Rényi random network topology attributes.
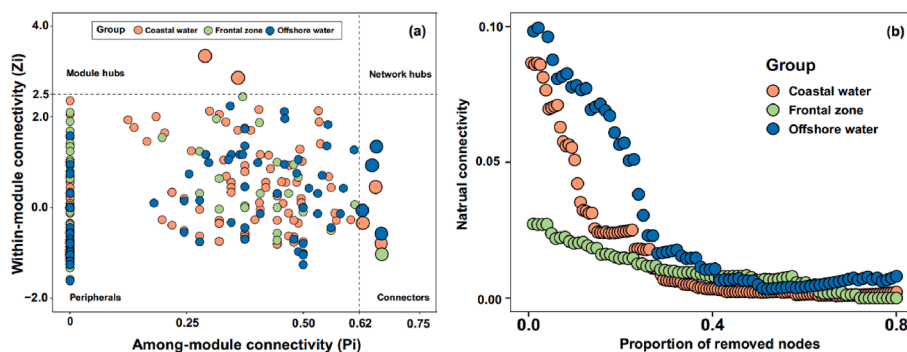
Fig. 4. Keystone taxa and robustness analysis for microbial co-occurrence networks of coastal water, frontal zone, and offshore water. (a) Keystone taxa are identified into peripherals, modular hubs, network hubs, or connectors based on the node topological roles in networks of coastal water, frontal zone, and offshore water. (b) The robustness of different networks is expressed by natural connectivity after removing a certain proportion of nodes.
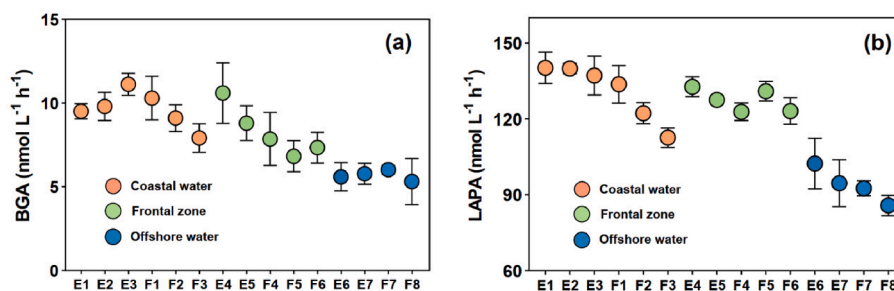
Fig. 5. Hydrolysis rate of extracellular activities at 15 stations in the middle of Taiwan Strait. (a) β-glucosidase activities. (b) leucine aminopeptidase activities.

further verified that this distinction was statistically significant ($P <$ 0.001) (Fig. 2c).

The diversity indices of the bacterial community based on Shannon diversity, Chao1 richness, and Pielou evenness all decreased from the coastal water to the frontal zone to the offshore water (Table S1). Specifically, compared with the frontal zone, the Shannon, Chao 1, and Pielou indices of the bacterial community in the offshore water decreased by 19.9% (Wilcoxon test, $P < 0.001$), 19.2% (Wilcoxon test, $P < 0.05$), and 16.0% (Wilcoxon test, $P < 0.05$), respectively (Table S1).

3.3. Bacterial co-occurrence networks

A co-occurrence network was constructed for each water mass based on the strong correlations among OTUs (Fig. 3a). All three networks showed a scale-free feature (power law: the R^2 of the coastal water, the frontal zone, and the offshore water were 0.89, 0.92, and 0.87,

respectively) (Table 1), the suggestion being that the organization of these ecological networks was non-random. The modularity value, average clustering coefficient, and average path length were significantly larger for all empirical networks than for the corresponding random networks, the indication being that the constructed networks had modular structures and small-world characteristics. The results of the basic structure of all networks showed that the network in the frontal zone differed from the other two networks (Table 1). The 175 shared edges in the frontal zone network were much lower than the 664 edges in the coastal water network and the 333 edges in the offshore water network (Table 1). In addition, the network of the frontal zone exhibited the highest modularity and the lowest average clustering coefficient (Table 1). Examination of the node-level topological properties revealed that the frontal zone network had the lowest node-level degree, closeness centrality, and eigenvector centrality (Fig. 3b). Importantly, there was only one keystone node in the frontal zone network, five in the
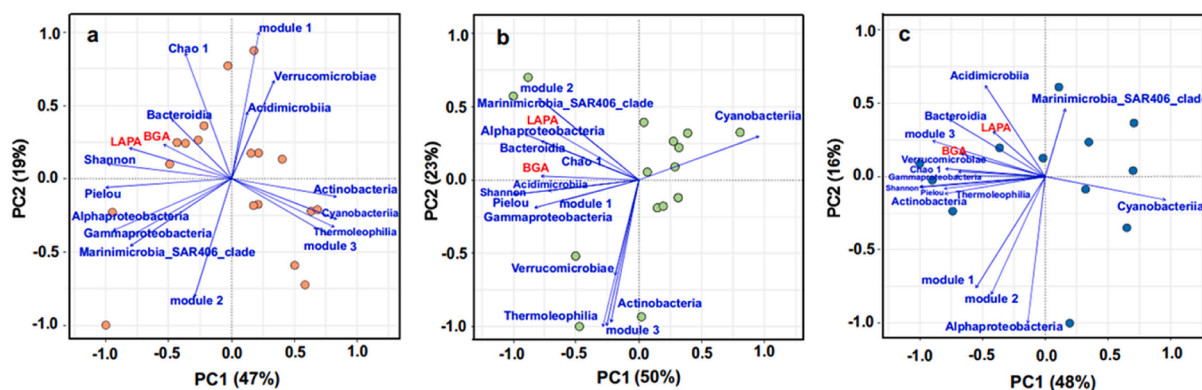
Fig. 6. Principal component analysis (PCA) shows the linkage between the EEA and shifts in the properties of the bacterial community (diversity, the relative abundance of dominant class-level taxa, as well as the relative abundance of the three main ecological clusters in the co-occurrence network) among the coastal water (a), frontal zone (b), and offshore water (c).
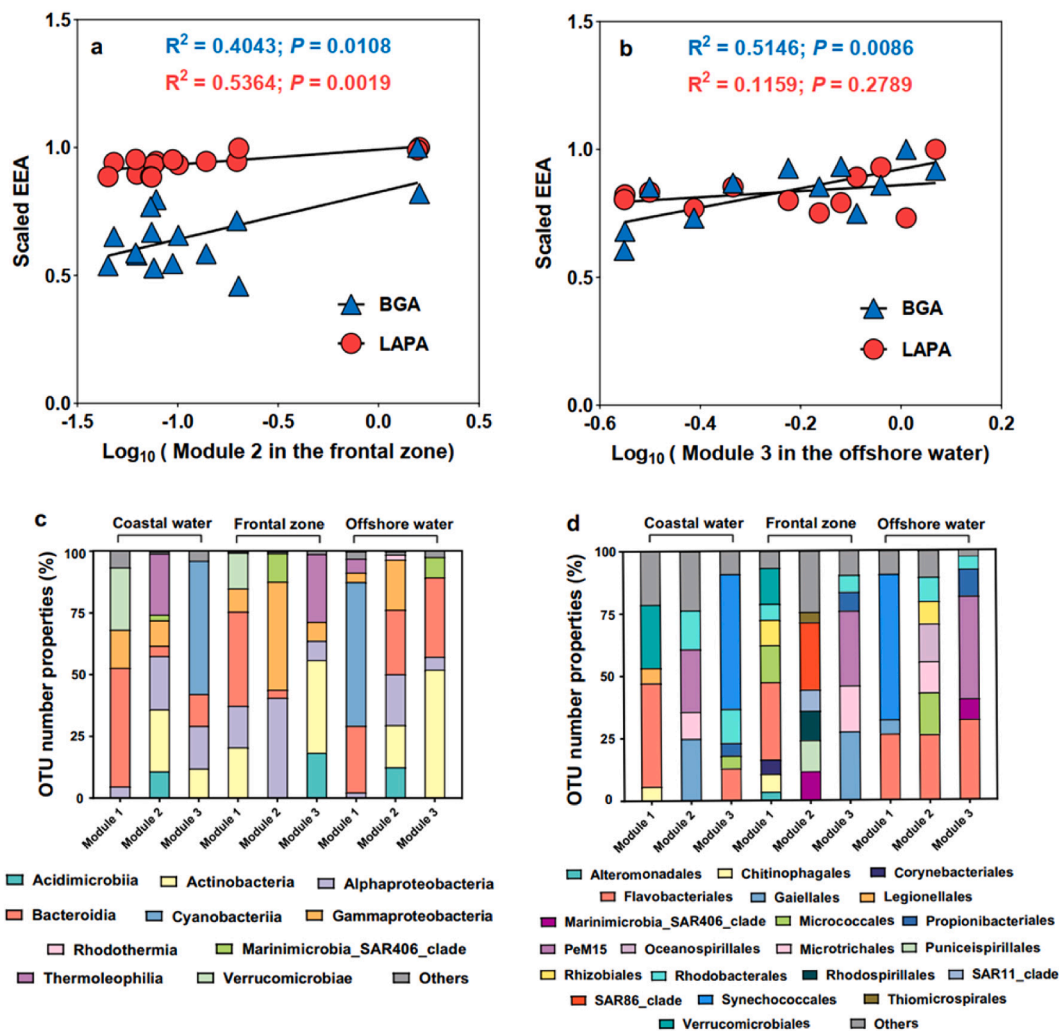
Fig. 7. Regressions between the scaled EEA (value divided by the maximum of all values) and the relative abundance of Module 2 in the frontal zone (a) and Module 3 in the offshore water (b) (only significant cases are shown in the figures). Operational taxonomic unit (OTU) number properties of the dominant class (c) and order (d) level taxa in the three main ecological clusters among the coastal water, frontal zone, and offshore water.

coastal zone network, and four in the offshore water network (Fig. 4a). Furthermore, the natural connectivity of the frontal zone network was significantly lower than that of the coastal water and offshore water, even when a small proportion of network nodes were removed (Fig. 4b). The indication was that the frontal zone network had the lowest robustness, i.e., its network structure was the most vulnerable to destruction.

3.4. Distribution pattern of EEA

We observed similar distribution patterns of BGA and LAPA among the three water masses (Fig. 5). Interestingly, the BGA and LAPA in the frontal zone (8.3 ± 1.7 nmol $L^{-1}h^{-1}$ and 127.5 ± 11.2 nmol $L^{-1}h^{-1}$, respectively) were both identical (Wilcoxon test, $P > 0.05$) with those in the coastal water (9.6 ± 1.2 nmol $L^{-1}h^{-1}$ and 131.0 ± 5.0 nmol $L^{-1}h^{-1}$, respectively, Fig. 5). Compared with the frontal zone, the BGA and LAPA in the offshore water (5.7 ± 0.8 nmol $L^{-1}h^{-1}$ and 92.8 ± 8.2 nmol $L^{-1}h^{-1}$) significantly decreased by 31.4% and 27.2%, respectively (Wilcoxon test, $P < 0.05$, Fig. 5).

3.5. Relationships between EEA and bacterial community structure

A PCA was conducted for each water mass to elucidate the relationships between the EEA and the properties of the bacterial community structure (Fig. 6). The first two principal axes explained 66%, 73%, and 64% of the cumulative percentage variance for the coastal water, the frontal zone, and the offshore water, respectively. For the dominant taxa, the relative abundances of Bacteroidia, Alphaproteobacteria, and Gammaproteobacteria were positively correlated with BGA and LAPA in all three water masses (Fig. 6). In the frontal zone, the relative abundances of Acidimicrobiia and Marinimicrobia_SAR406_clade were also potential drivers of the variations of the BGA and LAPA (Fig. 6b). In the offshore water, the relative abundances of Actinobacteria, Thermoleophilla, and Verrucomicrobiae were positively associated with BGA and LAPA (Fig. 6c). Two bacterial diversity indices, Shannon and Pielou, were positively correlated with BGA and LAPA in all three water masses (Fig. 6).

We explored the relationship between EEA and the relative abundance of the top three key microbial assemblages with the highest number of nodes in each network. Significant positive associations between the relative abundance of module 2 and EEA in the frontal zone were determined from both the PCA (Fig. 6b) and the linear regression analysis (BGA: $R^2 = 0.4043$, $P < 0.05$; LAPA: $R^2 = 0.5364$, $P < 0.01$) (Fig. 7a). The key assemblages for community composition of Module 2 in this water mass were dominated by Gammaproteobacteria (43.77%) and Alphaproteobacteria (40.67%) at the class level (Fig. 7c) and by SAR86_clade (26.99%), Puniceispirillales (12.47%), Rhodospirillales (11.79%), and Marinimicrobia_SAR406_clade (11.59%) at the order

level (Fig. 7d). A strong and significant positive correlation between the relative abundance of module 3 and BGA in the offshore water was found ($R^2 = 0.5146$, $P < 0.01$) (Fig. 6c and Fig. 7b). The dominant bacterial assemblages in module 3 of this water mass were Actinobacteria (52.03%) and Bacteroidia (32.18%) at the class level (Fig. 7c) and PeM15 (41.06%) and Flavobacteriales (32.18%) at the order level (Fig. 7d).

4. Discussion

4.1. Coastal fronts: Transition zones of bacterial composition and diversity

Ecotones in terrestrial systems are generally regarded as biodiversity hotspots (Smith et al., 1997; Kark, 2013; Morales et al., 2018). Fronts in the ocean are analogs of ecotones in terrestrial systems. However, in terms of bacterial diversity, the coastal front in our study functioned as a transition zone, not as a hotspot (Table S1). The compositions of bacterial communities differed greatly between water masses on the opposite sides of a frontal zone (Fig. 2a). Physical mixing of species from both sides of the front will therefore inevitably increase biodiversity in the front. However, the diversity of species within a coastal front may involve more than just physical mixing.

Several studies have focused on whether oceanic fronts are hotspots of planktonic (including bacterial) diversity, but the conclusions have differed. A previous study has shown that the permanent front in the Southern Ocean increases nutrient concentrations that subsequently enhance primary productivity and support a hotspot in the diversity of the bacterial community (Raes et al., 2018). However, in the present study, the effect of the gradients associated with the front on bacterial community diversity was similar to that of the gradients in the subtropical fronts along the New Zealand coast (Morales et al., 2018). This similarity might have resulted from the fact that the coastal front experienced continuous mixing, expansion, and contraction events that resulted in a highly fluctuating environment that was less stable than that of terrestrial ecotones (Morales et al., 2018). The coastal front was therefore not suitable for some of the specialized species that came from either the coastal or offshore waters. The coastal waters were dominated by typical freshwater phyla such as Actinobacteria and Bacteroidota (Fig. 2a) (Tamames et al., 2010; Zeglin, 2015), whereas the offshore water was dominated by the phylum Cyanobacteria (Fig. 2a), which includes species found in both freshwater and marine habitats (Biller et al., 2015). The front also functioned as a transition zone in terms of bacterial community composition, but the community tended to be similar to that found in the offshore waters (Fig. 2a). These results suggested that the dramatic change in the environment of the frontal zone may have created conditions that made it difficult for some of the specialized species from coastal waters to adapt to the osmotic stress (Mo et al., 2021a; Taylor and Cunliffe, 2016). Our findings support the basic concept that the biodiversity in habitats with large spatiotemporal fluctuations is lower than that in habitats characterized by long-term stability (Morales et al., 2018).

4.2. Coastal fronts reduce the complexity and stability of bacterial co-occurrence networks

It is generally accepted that environmental heterogeneity reduces the complexity of the co-occurrence patterns of microbes in terrestrial ecosystems (Gao et al., 2022; Mo et al., 2021a; Qiu et al., 2021), but it is unclear whether this pattern holds true in marine ecosystems. We found that the interactions of bacterial communities in a highly heterogeneous front in the TS were characterized by the lowest node-level average degree, closeness centrality, and eigenvector centrality among the three water masses (Fig. 3b). These results demonstrated that the network was much simpler and more discrete in the frontal zone than in the coastal and offshore water masses (Zhang et al., 2021). The reason may be that

the abrupt environmental changes in the front created strong selective pressure on the bacterial communities that excluded some microorganisms from the network and led to a simpler network (Ratzke et al., 2020). Our results therefore suggested that the phenomenon of environmental heterogeneity's reducing co-occurrence complexity may be common to both terrestrial and marine ecosystems. The indication is that reducing interaction complexity is a basic adaptive response of microbial communities to drastic changes in the environment.

Our results also support the general view that more complex (simpler) network structures may be associated with more stable (unstable) coexistence patterns (Mo et al., 2021b). We found that in the frontal zone the natural connectivity was the lowest and the number of keystone species the fewest among the three water masses (Fig. 4). The low natural connectivity of the frontal zone network (Fig. 4b) indicated that the interactions of the bacterial community were vulnerable to the "stress" of environmental variations in the frontal zone. This vulnerability led to a relatively low level of robustness in their co-occurrence relationships (Mo et al., 2021a). Because keystone taxa are generally considered to be the drivers in shaping network structure (Banerjee et al., 2018; Liu et al., 2022; Yuan et al., 2021), the sharp decrease in the number of keystone taxa (Fig. 4a) in the frontal zone also reflected the simplicity and instability of the entire co-occurrence pattern.

4.3. Potential mechanisms that control EEA

Understanding the carbon cycling capacity of microbial communities in the ocean requires identification of the complex linkages between microbial community structure and hydrolysis capacity (D'Ambrosio et al., 2014; Louca et al., 2018; Shi et al., 2019). In the present study, the levels of BGA and LAPA were as high in the frontal zone as in the coastal water, and were obviously higher than those in the offshore water (Fig. 5). Because the bacterial beta-diversity declined from the coastal water to the frontal zone to the offshore water (Fig. 2b) whereas complexity and stability were lowest in the frontal zone, the linkages between the bacterial community structure and EEA across the frontal zone appeared to be complex.

Bacterial EEA tells us not only how active these microbes are but also how diverse the organic substrates are that they use (Baltar and Aristegui, 2017). The BG and LAP assayed in this study are used to cleave the β (1–4) glycosidic linkages of complex carbohydrates and peptides in proteins, respectively (Caruso, 2010; Caruso and Zaccone, 2000). The west coast of the TS is strongly influenced by land-based organic matter driven by the Zhe-Min Coastal Current (Lin et al., 2016). High loadings of organic matter can stimulate bacterial EEA (Caruso, 2010; Celussi and Del Negro, 2012), and high values of BGA and LAPA in the coastal water (Fig. 5a and 5b) indicated that polysaccharides and polymers derived from proteins were being produced. DOM produced by planktonic sources can stimulate bacterial EEA (Caruso, 2010; Shi et al., 2019), and proteins are the major components of biogenic organic matter. The fact that BGA and LAPA were as high in the frontal zone as in the coastal water (Fig. 5) and the Chl *a* concentrations were highest in the frontal zone (Fig. S1f) suggested that the high phytoplankton biomass that accumulated in the frontal zone may have supplied unstable and freshly produced proteins to bacterioplankton and stimulated high levels of EEA (Caruso and Zaccone, 2000).

The PCA results revealed that the BGA and LAPA were positively correlated with the Shannon and Pielou indices in all three water masses (Fig. 6). The suggestion was that bacterial diversity was likely a key factor in the regulation of enzymatic activity. Of particular note is the fact that the relative abundances of the classes of Bacteroidia, Gammaproteobacteria, and Alphaproteobacteria were positively correlated with BGA and LAPA in all three water masses, the indication being that these three groups included bacteria that expressed both enzymes (Fig. 6). The Bacteroidia are thought to be fast-growing r-strategists that specialize in degrading high-molecular-weight DOM in marine ecosystems (Fernandez-Gomez et al., 2013; Teeling et al., 2012; Thomas et al.,
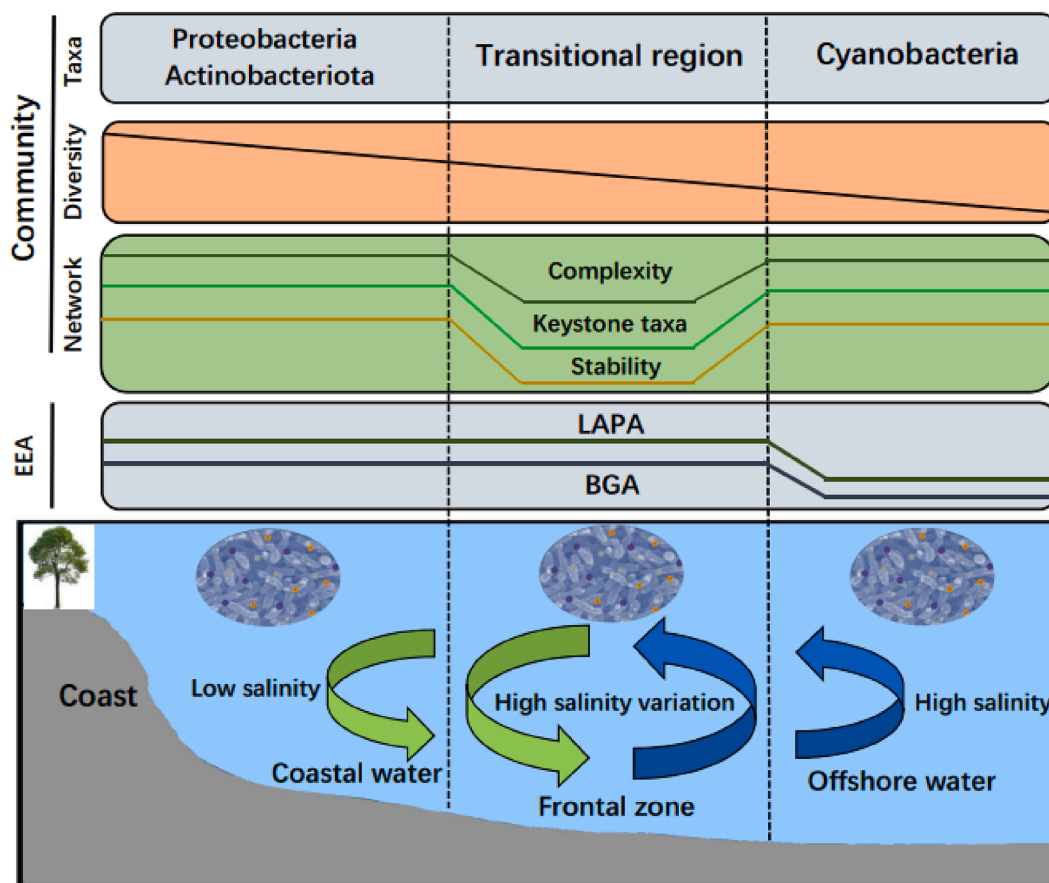
Fig. 8. Proposed conceptual models of bacterial dominant taxa, diversities, network properties, and EEA influenced by coastal salinity fronts.

2011). The Bacteroidetes may therefore include some of the most active cell groups with a particularly high affinity for DOM derived from diatoms and cyanobacteria (Sarmento and Gasol, 2012), and members of the Bacteroidetes may contain a large number of glycosidase and protease genes that enable them to preferentially exploit polymeric carbon sources (Bauer et al., 2006; Fernandez-Gomez et al., 2013). Gammaproteobacteria are also fast-growing opportunists and can rapidly adapt to salinity stress and changes of substrate availability (Eswaran and Khandeparker, 2020; Langenheder et al., 2003). Exopolymer enrichment studies have shown that the major genera of Gammaproteobacteria, Pantoea, and Acinetobacter, possess genes for BG production and polysaccharide degradation (Arora et al., 2012; Tajima et al., 2001). Similarly, Alphaproteobacteria possess carbohydrate-degrading capacity and have been found to be associated with BGA expression in tropical monsoon-affected estuarine regions (Eswaran and Khandeparker, 2020; Teeling et al., 2012). Note that although some microbes are specialized in expressing one extracellular enzyme, the close relationship between the BGA and LAPA (Fig. 6) suggested that degradation of glycosides and oligosaccharides was unlikely to be greater than that of peptides and proteins because different types of compounds (such as monosaccharides and amino acids) required for microbial metabolism may often be in a polymeric state (Caruso, 2010; Hoppe and Ullrich, 1999).

Functional redundancy of enzymatic capacity occurs when different groups of bacterial taxa share the ability to use the same substrate (D'Ambrosio et al., 2014). In our study, the microbial community in the frontal zone was characterized by a different composition, lower diversity, and weaker interactions than the microbial community in the coastal water, but the fact that the BGA and LAPA were still high implied that there may have been functional redundancy of enzymatic capabilities in the frontal zone. Indeed, bacterioplankton tend to change their mineralization pathways under different environmental conditions, and

changes of salinity can be considered to be stressors of bacterial physiological states and functional activities (del Giorgio and Bouvier, 2002; Eswaran and Khandeparker, 2020). Functional redundancies of bacterial communities have been reported in other studies. For instance, two communities with different compositions in the surface and bottom water of an Arctic fjord have been found to show similar extracellular enzymatic hydrolysis capabilities for 10 substrates (polysaccharides and algal extracts) (Teske et al., 2011). Also, bacterial communities at different water depths off the coast of North Carolina are able to hydrolyze a similar set of substrates, including six polysaccharides, despite low community overlap (D'Ambrosio et al., 2014).

The fact that microbial communities in distinctly different habitats can be classified into assemblages with specific trait combinations based on differences in the co-occurrence or association patterns of those traits provides new insights into the community structure and ecological functions of complex microbial communities (Fan et al., 2019; Feng et al., 2021). Intriguingly, the increase of BGA and LAPA in the frontal zone with the relative abundance of module 2 (Fig. 7a) suggested that these highly connected taxa had adapted to abrupt changes in the environment and substrate quality. In the frontal zone, the largest taxon in module 2 was the SAR86_clade at the order level (Fig. 7d). This taxon belongs to the Gammaproteobacteria (Fig. 7c), which is widely distributed on the ocean surface and has been shown to have the ability to adapt to changes in salinity (Zhou et al., 2018; Zubkov et al., 2002). Genomic analysis has demonstrated that the SAR86_clade contains multiple carbohydrate-degrading enzymes and peptidases and that it participates in DOM cycling through the use of polysaccharides and leucine (Dupont et al., 2012; Teira et al., 2017). In the offshore water, the BGA was positively correlated with the relative abundance of module 3 (Fig. 7b), which was composed mainly of PeM15 within the Actinobacteria and Flavobacteriales within the Bacteroidia (Fig. 7c and

7d). Actinobacteria can promote the turnover of complex biopolymers by synthesizing a variety of enzymes (Gonzalez et al., 2020), and a significant correlation between Actinobacteria and BGA gene abundance has been found in tidal estuaries (Eswaran and Khandeparker, 2017). A previous study has also found that Flavobacteriales are the main producers of BGA during the monsoon period in a tropical estuary (Eswaran and Khandeparker, 2019). Together, these results imply that it is likely that changes in bacterial assemblages in a dynamic frontal zone strongly affect EEA functions.

5. Conclusion

In this study, we investigated the composition, diversity, and co-occurrence networks of the bacterial community on the west coast of the TS in the late spring of 2020, and we determined the activities of two extracellular enzymes. We divided the study area into three water masses based on salinity: coastal water, offshore water, and a frontal zone between them. We found that the coastal front functioned as a transitional zone rather than a hotspot for the transformation of the bacterial community composition and diversity from the coastal water to the offshore water. The co-occurrence network in the frontal zone showed the lowest complexity indices, including node-level average degree, closeness centrality, and eigenvector centrality, among the three water masses. Stability indicators such as natural connectivity and the number of keystone taxa were also the lowest in the frontal zone. The distribution patterns of EEA showed that the BGA and LAPA were as high in the coastal water and frontal zone. These results suggest that coastal fronts strongly delineate biogeochemically distinct zones and that the front significantly altered the linkage between bacterial communities and EEA (Fig. 8). We also found that the functional redundancy of EEA, was likely a key trait for simple, unstable communities in highly dynamic frontal zones that allowed them to realize their mineralization functions. Moreover, the significant, positive correlation between the relative abundance of module 2 in the frontal zone and EEA suggested that a change of the bacterial assemblage pattern is a potential mechanism for maintaining EEA in the frontal zone. Our findings have deepened our understanding of the community-function relationship of bacterioplankton in fluctuating ocean environments.

CRediT authorship contribution statement

Shujie Cai: Investigation, Data curation, Visualization, Writing – original draft, Writing – review & editing. **Feipeng Wang:** Writing – review & editing. **Edward A. Laws:** Methodology, Writing – review & editing. **Yao Liu:** Methodology, Formal analysis. **Chao Xu:** Methodology, Visualization. **Lingqi Ma:** Methodology, Data curation. **Wupeng Xiao:** Conceptualization, Methodology, Investigation, Funding acquisition, Writing – review & editing. **Bangqin Huang:** Conceptualization, Methodology, Investigation, Funding acquisition, Writing – review & editing.

Declaration of Competing Interest

The authors declare that they have no known competing financial interests or personal relationships that could have appeared to influence the work reported in this paper.

Data availability

Sequencing data of all samples can be found at the NCBI with SRA accession number PRJNA856774.

Acknowledgments

Appendix A. Supplementary data

Supplementary data to this article can be found online at https://doi.org/10.1016/j.ecolind.2022.109639.

References

Allen, R., Summerfield, T.C., Currie, K., Dillingham, P.W., Hoffmann, L.J., 2020. Distinct processes structure bacterioplankton and protist communities across an oceanic front. Aquat. Microb. Ecol. 85, 19–34.

Arnosti, C., 2011. Microbial extracellular enzymes and the marine carbon cycle. Ann. Rev. Marine Sci. 3, 401–425.

Arora, M., Anil, A.C., Delany, J., Rajarajan, N., Emami, K., Mesbahi, E., 2012. Carbohydrate-degrading bacteria closely associated with Tetraselmis indica: influence on algal growth. Aquat. Biol. 15 (1), 61–71.

Azam, F., Malfatti, F., 2007. Microbial structuring of marine ecosystems. Nat. Rev. Microbiol. 5 (10), 782–791.

Baltar, F., Aristegui, J., 2017. Fronts at the surface ocean can shape distinct regions of microbial activity and community assemblages down to the bathypelagic zone: The Azores Front as a case study. Front. Mar. Sci. 4, 252.

Baltar, F., Currie, K., Stuck, E., Roosa, S., Morales, S.E., 2016. Oceanic fronts: transition zones for bacterioplankton community composition. Environ. Microbiol. Rep. 8 (1), 132–138.

Banerjee, S., Baah-Acheamfour, M., Carlyle, C.N., Bissett, A., Richardson, A.E., Siddique, T., Bork, E.W., Chang, S.X., 2016. Determinants of bacterial communities in Canadian agroforestry systems. Environ. Microbiol. 18 (6), 1805–1816.

Banerjee, S., Schlaeppi, K., van der Heijden, M.G.A., 2018. Keystone taxa as drivers of microbiome structure and functioning. Nat. Rev. Microbiol. 16 (9), 567–576.

Barbier, E.B., Hacker, S.D., Kennedy, C., Koch, E.W., Stier, A.C., Silliman, B.R., 2011. The value of estuarine and coastal ecosystem services. Ecol. Monogr. 81 (2), 169–193.

Bauer, M., Kube, M., Teeling, H., Richter, M., Lombardot, T., Allers, E., Wuerdemann, C. A., Quast, C., Kuhl, H., Knaust, F., Woebken, D., Bischof, K., Mussmann, M., Choudhuri, J.V., Meyer, F., Reinhardt, R., Amann, R.I., Gloeckner, F.O., 2006. Whole genome analysis of the marine Bacteroidetes 'Gramella forsetii' reveals adaptations to degradation of polymeric organic matter. Environ. Microbiol. 8 (12), 2201–2213.

Belkin, I.M., Cornillon, P.C., Sherman, K., 2009. Fronts in large marine ecosystems. Prog. Oceanogr. 81 (1–4), 223–236.

Biller, S.J., Berube, P.M., Lindell, D., Chisholm, S.W., 2015. Prochlorococcus: the structure and function of collective diversity. Nat. Rev. Microbiol. 13 (1), 13–27.

Buchan, A., LeCleir, G.R., Gulvik, C.A., Gonzalez, J.M., 2014. Master recyclers: features and functions of bacteria associated with phytoplankton blooms. Nat. Rev. Microbiol. 12 (10), 686–698.

Caporaso, J.G., Kuczynski, J., Stombaugh, J., Bittinger, K., Bushman, F.D., Costello, E.K., Fierer, N., Pena, A.G., Goodrich, J.K., Gordon, J.I., Huttley, G.A., Kelley, S.T., Knights, D., Koenig, J.E., Ley, R.E., Lozupone, C.A., McDonald, D., Muegge, B.D., Pirrung, M., Reeder, J., Sevinsky, J.R., Tumbaugh, P.J., Walters, W.A., Widmann, J., Yatsunenko, T., Zaneveld, J., Knight, R., 2010. QIIME allows analysis of high-throughput community sequencing data. Nat. Methods 7 (5), 335–336.

Caruso, G., 2010. Leucine aminopeptidase, β-glucosidase and alkaline phosphatase activity rates and their significance in nutrient cycles in some coastal Mediterranean sites. Mar. Drugs 8 (4), 916–940.

Caruso, G., Zaccone, R., 2000. Estimates of leucine aminopeptidase activity in different marine and brackish environments. J. Appl. Microbiol. 89 (6), 951–959.

Celussi, M., Del Negro, P., 2012. Microbial degradation at a shallow coastal site: Long-term spectra and rates of exoenzymatic activities in the NE Adriatic Sea, Estuarine. Coast. Shelf Sci. 115, 75–86.

D'Ambrosio, L., Ziervogel, K., MacGregor, B., Teske, A., Arnosti, C., 2014. Composition and enzymatic function of particle-associated and free-living bacteria: a coastal/offshore comparison. ISME J. 8 (11), 2167–2179.

del Giorgio, P.A., Bouvier, T.C., 2002. Linking the physiologic and phylogenetic successions in free-living bacterial communities along an estuarine salinity gradient. Limnol. Oceanogr. 47 (2), 471–486.

Dupont, C.L., Rusch, D.B., Yooseph, S., Lombardo, M.-J., Richter, R.A., Valas, R., Novotny, M., Yee-Greenbaum, J., Selengut, J.D., Haft, D.H., Halpern, A.L., Lasken, R. S., Nealson, K., Friedman, R., Venter, J.C., 2012. Genomic insights to SAR86, an abundant and uncultivated marine bacterial lineage. ISME J. 6 (6), 1186–1199.

Edgar, R.C., 2013. UPARSE: highly accurate OTU sequences from microbial amplicon reads. Nat. Methods 10 (10), 996–998.

Erdős, P., 1960. On sets of distances of n points in Euclidean space. Magyar Tudom. Akad. Matem. Kut. Int. Közl. Publ. Math. Inst. Hung. Acad. Sci. 5, 165–169.

Eswaran, R., Khandeparker, L., 2017. Seasonal variation in bacterial community composition and β-glucosidase expression in a tropical monsoon-influenced estuary. Aquat. Microb. Ecol. 80 (3), 273–287.

Eswaran, R., Khandeparker, L., 2019. Seasonal variation in β-glucosidase-producing culturable bacterial diversity in a monsoon-influenced tropical estuary. Environ. Monit. Assess. 191 (11), 1–11.

Eswaran, R., Khandeparker, L., 2020. Influence of salinity stress on bacterial community composition and β-glucosidase activity in a tropical estuary: Elucidation through microcosm experiments. Marine Environ. Res. 159, 104997.

Fan, K., Delgado-Baquerizo, M., Guo, X., Wang, D., Wu, Y., Zhu, M., Yu, W., Yao, H., Zhu, Y., Chu, H., 2019. Suppressed N fixation and diazotrophs after four decades of fertilization. Microbiome 7 (1), 1–10.

Faust, K., Raes, J., 2012. Microbial interactions: from networks to models. Nat. Rev. Microbiol. 10 (8), 538–550.

Feng, J., Zeng, X.M., Zhang, Q., Zhou, X.Q., Liu, Y.R., Huang, Q., 2021. Soil microbial trait-based strategies drive metabolic efficiency along an altitude gradient. ISME Commun. 1 (1), 1–9.

Fernandez-Gomez, B., Richter, M., Schueler, M., Pinhassi, J., Acinas, S.G., Gonzalez, J. M., Pedros-Alio, C., 2013. Ecology of marine Bacteroidetes: a comparative genomics approach. ISME J. 7 (5), 1026–1037.

Friedman, J., Alm, E.J., 2012. Inferring correlation networks from genomic survey data. PLoS Comput. Biol. 8, 1–11.

Gao, G.F., Li, H., Shi, Y., Yang, T., Gao, C.H., Fan, K., Zhang, Y., Zhu, Y.G., Delgado-Baquerizo, M., Hai-Lei, Z., Chu, H., 2022. Continental-scale plant invasions reshuffle the soil microbiome of blue carbon ecosystems. Glob. Change Biol. 28, 4423–4438.

Gildor, H., Fredj, E., Steinbuck, J., Monismith, S., 2009. Evidence for submesoscale barriers to horizontal mixing in the ocean from current measurements and aerial photographs. J. Phys. Oceanogr. 39 (8), 1975–1983.

Gonzalez, V., Vargas-Straube, M.J., Beys-da-Silva, W.O., Santi, L., Valencia, P., Beltrametti, F., Camara, B., 2020. Enzyme bioprospection of marine-derived Actinobacteria from the Chilean Coast and new insight in the mechanism of keratin degradation in Streptomyces sp. G11C. Mar. Drugs 18 (11), 537.

Hong, H., Chai, F., Zhang, C., Huang, B., Jiang, Y., Hu, J., 2011. An overview of physical and biogeochemical processes and ecosystem dynamics in the Taiwan Strait. Cont. Shelf Res. 31 (6), S3–S12.

Hoppe, H.G., 1983. Significance of exoenzymatic activities in the ecology of brackish water: measurements by means of methylumbelliferyl-substrates. Mar. Ecol. Prog. Ser. 11 (3), 299–308.

Hoppe, H.G., Ullrich, S., 1999. Profiles of ectoenzymes in the Indian Ocean: phenomena of phosphatase activity in the mesopelagic zone. Aquat. Microb. Ecol. 19 (2), 139–148.

Kark, S., 2013. Ecotones and ecological gradients. In: Leemans, R. (Ed.), Ecological Systems. Springer, New York, pp. 147–160.

Kellogg, C.T.E., Deming, J.W., 2014. Particle-associated extracellular enzyme activity and bacterial community composition across the Canadian Arctic Ocean. FEMS Microbiol. Ecol. 89 (2), 360–375.

Langenheder, S., Kisand, V., Wikner, J., Tranvik, L.J., 2003. Salinity as a structuring factor for the composition and performance of bacterioplankton degrading riverine DOC. FEMS Microbiol. Ecol. 45 (2), 189–202.

Lefcheck, J.S., Orth, R.J., Dennison, W.C., Wilcox, D.J., Murphy, R.R., Keisman, J., Gurbisz, C., Hannam, M., Landry, J.B., Moore, K.A., Patrick, C.J., Testa, J., Weller, D. E., Batiuk, R.A., 2018. Long-term nutrient reductions lead to the unprecedented recovery of a temperate coastal region. Proc. Natl. Acad. Sci. 115 (14), 3658–3662.

Li, W., Ge, J., Ding, P., Ma, J., Glibert, P.M., Liu, D., 2021. Effects of dual fronts on the spatial pattern of chlorophyll-a concentrations in and off the Changjiang River Estuary. Estuaries Coasts 44 (5), 1408–1418.

Li, C., Hu, J., Jan, S., Wei, Z., Fang, G., Zheng, Q., 2006. Winter-spring fronts in Taiwan Strait. J. Geophys. Res. Oceans 111 (C11).

Li, Y., Sun, L.L., Sun, M.L., Su, H.N., Zhang, X.Y., Xie, B.B., Chen, X.L., Zhang, Y.Z., Qin, Q.L., 2018. Vertical and horizontal biogeographic patterns and major factors affecting bacterial communities in the open South China Sea. Sci. Rep. 8 (1), 1–10.

Liao, E., Oey, L.Y., Yan, X.-H., Li, L., Jiang, Y., 2018. The deflection of the China Coastal Current over the Taiwan Bank in winter. J. Phys. Oceanogr. 48 (7), 1433–1450.

Lin, H., Cai, Y., Sun, X., Chen, G., Huang, B., Cheng, H., Chen, M., 2016. Sources and mixing behavior of chromophoric dissolved organic matter in the Taiwan Strait. Mar. Chem. 187, 43–56.

Liu, R., Wang, L., Liu, Q., Wang, Z., Li, Z., Fang, J., Li, Z., Min, L., 2018. Depth-resolved distribution of particle-attached and free-living bacterial communities in the water column of the New Britain Trench. Front. Microbiol. 9, 625.

Liu, S., Yu, H., Yu, Y., Huang, J., Zhou, Z., Zeng, J., Chen, P., Xiao, F., He, Z., Yan, Q., 2022. Ecological stability of microbial communities in Lake Donghu regulated by keystone taxa. Ecol. Ind. 136, 108695.

Louca, S., Polz, M.F., Mazel, F., Albright, M.B.N., Huber, J.A., O'Connor, M.I., Ackermann, M., Hahn, A.S., Srivastava, D.S., Crowe, S.A., Doebeli, M., Parfrey, L.W., 2018. Function and functional redundancy in microbial systems. Nat. Ecol. Evol. 2 (6), 936–943.

Lurgi, M., Thomas, T., Wemheuer, B., Webster, N.S., Montoya, J.M., 2019. Modularity and predicted functions of the global sponge-microbiome network. Nat. Commun. 10 (1), 1–12.

McGillicuddy, D.J., 2016. Mechanisms of physical-biological-biogeochemical interaction at the oceanic mesoscale. Annu. Rev. Marine Sci. 8 (1), 125–159.

Mo, Y., Peng, F., Gao, X., Xiao, P., Logares, R., Jeppesen, E., Ren, K., Xue, Y., Yang, J., 2021a. Low shifts in salinity determined assembly processes and network stability of microeukaryotic plankton communities in a subtropical urban reservoir. Microbiome 9 (1), 1–17.

Mo, Y., Zhang, W., Wilkinson, D.M., Yu, Z., Xiao, P., Yang, J., 2021b. Biogeography and co-occurrence patterns of bacterial generalists and specialists in three subtropical marine bays. Limnol. Oceanogr. 66 (3), 793–806.

Monticelli, L.S., Caruso, G., Decembrini, F., Caroppo, C., Fiesoletti, F., 2014. Role of prokaryotic biomasses and activities in carbon and phosphorus cycles at a coastal, thermohaline front and in offshore waters (Gulf of Manfredonia, Southern Adriatic Sea). Microb. Ecol. 67 (3), 501–519.

Morales, S.E., Meyer, M., Currie, K., Baltar, F., 2018. Are oceanic fronts ecotones? Seasonal changes along the subtropical front show fronts as bacterioplankton transition zones but not diversity hotspots. Environ. Microbiol. Rep. 10 (2), 184–189.

Olesen, J.M., Bascompte, J., Dupont, Y.L., Jordano, P., 2007. The modularity of pollination networks. Proceedings of the National Academy of Sciences 104 (50), 19891–19896.

Peng, G.S., Wu, J., 2016. Optimal network topology for structural robustness based on natural connectivity. Physica A 443, 212–220.

Qiu, L., Zhang, Q., Zhu, H., Reich, P.B., Banerjee, S., van der Heijden, M.G.A., Sadowsky, M.J., Ishii, S., Jia, X., Shao, M., Liu, B., Jiao, H., Li, H., Wei, X., 2021. Erosion reduces soil microbial diversity, network complexity and multifunctionality. ISME J. 15 (8), 2474–2489.

Raes, E.J., Bodrossy, L., van de Kamp, J., Bissett, A., Ostrowski, M., Brown, M.V., Sow, S. L.S., Sloyan, B., Waite, A.M., 2018. Oceanographic boundaries constrain microbial diversity gradients in the South Pacific Ocean. Proceedings of the National Academy of Sciences 115 (35), E8266–E8275.

Ratzke, C., Barrere, J., Gore, J., 2020. Strength of species interactions determines biodiversity and stability in microbial communities. Nat. Ecol. Evol. 4 (3), 376–383.

Ribalet, F., Marchetti, A., Hubbard, K.A., Brown, K., Durkin, C.A., Morales, R., Robert, M., Swalwell, J.E., Tortell, P.D., Armbrust, E.V., 2010. Unveiling a phytoplankton hotspot at a narrow boundary between coastal and offshore waters. Proc. Natl. Acad. Sci. 107 (38), 16571–16576.

Sarmento, H., Gasol, J.M., 2012. Use of phytoplankton-derived dissolved organic carbon by different types of bacterioplankton. Environ. Microbiol. 14 (9), 2348–2360.

Shi, Z., Xu, J., Li, X., Li, R., Li, Q., 2019. Links of extracellular enzyme activities, microbial metabolism, and community composition in the river-impacted coastal waters. J. Geophys. Res. Biogeosci. 124 (11), 3507–3520.

Smith, T.B., Wayne, R.K., Girman, D.J., Bruford, M.W., 1997. A role for ecotones in generating rainforest biodiversity. Science 276, 1855–1857.

Steele, J.A., Countway, P.D., Xia, L., Vigil, P.D., Beman, J.M., Kim, D.Y., Chow, C.-E.-T., Sachdeva, R., Jones, A.C., Schwalbach, M.S., Rose, J.M., Hewson, I., Patel, A., Sun, F., Caron, D.A., Fuhrman, J.A., 2011. Marine bacterial, archaeal and protistan association networks reveal ecological linkages. ISME J. 5 (9), 1414–1425.

Tajima, K., Nakajima, K., Yamashita, H., Shiba, T., Munekata, M., Takai, M., 2001. Cloning and sequencing of the beta-glucosidase gene from *Acetobacter xylinum* ATCC 23769. DNA Res. 8 (6), 263–269.

Tamames, J., Jose Abellan, J., Pignatelli, M., Camacho, A., Moya, A., 2010. Environmental distribution of prokaryotic taxa. BMC Microbiol. 10 (1), 1–14.

Taylor, J.D., Cunliffe, M., 2016. Multi-year assessment of coastal planktonic fungi reveals environmental drivers of diversity and abundance. ISME J. 10 (9), 2118–2128.

Teeling, H., Fuchs, B.M., Becher, D., Klockow, C., Gardebrecht, A., Bennke, C.M., Kassabgy, M., Huang, S., Mann, A.J., Waldmann, J., Weber, M., Klindworth, A., Otto, A., Lange, J., Bernhardt, J., Reinsch, C., Hecker, M., Peplies, J., Bockelmann, F. D., Callies, U., Gerdts, G., Wichels, A., Wiltshire, K.H., Gloeckner, F.O., Schweder, T., Amann, R., 2012. Substrate-controlled succession of marine bacterioplankton populations induced by a phytoplankton bloom. Science 336 (6081), 608–611.

Teira, E., Hernando-Morales, V., Guerrero-Feijoo, E., Varela, M.M., 2017. Leucine, starch and bicarbonate utilization by specific bacterial groups in surface shelf waters off Galicia (NW Spain). Environ. Microbiol. 19 (6), 2379–2390.

Terhaar, J., Lauerwald, R., Regnier, P., Gruber, N., Bopp, L., 2021. Around one third of current Arctic Ocean primary production sustained by rivers and coastal erosion. Nat. Commun. 12 (1), 1–10.

Teske, A., Durbin, A., Ziervogel, K., Cox, C., Arnosti, C., 2011. Microbial community composition and function in permanently cold seawater and sediments from an Arctic fjord of Svalbard. Appl. Environ. Microbiol. 77 (6), 2008–2018.

Thomas, F., Hehemann, J.H., Rebuffet, E., Czjzek, M., Michel, G., 2011. Environmental and gut Bacteroidetes: the food connection. Front. Microbiol. 2, 93.

Welschmeyer, N.A., 1994. Fluorometric analysis of chlorophyll a in the presence of chlorophyll b and pheopigments. Limnol. Oceanogr. 39 (8), 1985–1992.

Wu, M., Chen, S., Chen, J., Xue, K., Chen, S., Wang, X., Chen, T., Kang, S., Rui, J., Thies, J., Bardgett, R.D., Wang, Y., 2021. Reduced microbial stability in the active layer is associated with carbon loss under alpine permafrost degradation. Proc. Natl. Acad. Sci. 118 (25) e2025321118.

Xu, Z., Li, Y., Lu, Y., Li, Y., Yuan, Z., Dai, M., Liu, H., 2020. Impacts of the Zhe-min coastal current on the biogeographic pattern of microbial eukaryotic communities. Prog. Oceanogr. 183, 102309.

Yuan, M.M., Guo, X., Wu, L., Zhang, Y., Xiao, N., Ning, D., Shi, Z., Zhou, X., Wu, L., Yang, Y., 2021. Climate warming enhances microbial network complexity and stability. Nat. Clim. Change 11 (4), 343–348.

Zeglin, L.H., 2015. Stream microbial diversity in response to environmental changes: review and synthesis of existing research. Front. Microbiol. 6, 454.

Zhang, L., Delgado-Baquerizo, M., Shi, Y., Liu, X., Yang, Y., Chu, H., 2021. Co-existing water and sediment bacteria are driven by contrasting environmental factors across glacier-fed aquatic systems. Water Res. 198, 117139.

Zhou, J., Song, X., Zhang, C.Y., Chen, G.F., Lao, Y.M., Jin, H., Cai, Z.H., 2018. Distribution patterns of microbial community structure along a 7000-mile latitudinal transect from the Mediterranean Sea across the Atlantic Ocean to the Brazilian Coastal Sea. Microb. Ecol. 76 (3), 592–609.

Zubkov, M.V., Fuchs, B.M., Tarran, G.A., Burkill, P.H., Amann, R., 2002. Mesoscale distribution of dominant bacterioplankton groups in the northern North Sea in early summer. Aquat. Microb. Ecol. 29 (2), 135–144.